Cascade effects on the Ar *LMM* Auger spectrum

J. W. Cooper,[1] S. H. Southworth,[2] M. A. MacDonald,[3] and T. LeBrun[4]
[1]*Institute for Physical Science and Technology, University of Maryland, College Park, Maryland 20742*
[2]*National Institute of Standards and Technology, Gaithersburg, Maryland 20899*
[3]*Science and Engineering Research Council, Daresbury Laboratory, Warrington WA4 4AD, United Kingdom*
[4]*Argonne National Laboratory, Argonne, Illinois 60439*
(Received 17 January 1994)

Generally, at excitation energies well above inner-shell ionization thresholds, Auger spectra are independent of the method of excitation. A notable exception to this has been found for the Ar $L_{2,3}MM$ Auger spectra where different results are obtained via electron-impact ionization at 2 and 4.5 keV and photoionization below the K edge at 3.17 and 2.2 keV. The differences are explained by the variation of the contribution of L_1 to $L_{2,3}$ vacancy transfers with the mode of excitation. Calculations using a simple vacancy transfer model explain the observed spectra.

PACS number(s): 32.80.Hd

I. INTRODUCTION

The $L_{2,3}MM$ Auger spectrum of argon has been the subject of a number of experimental and theoretical investigations over the past several decades [1]. The "normal" Auger spectrum, which arises from the decay of a single L_2 or L_3 vacancy, is known to consist in principle of 20 lines: 10 corresponding to decay of a $2p^5$ $(J=\frac{1}{2},\frac{3}{2})$ vacancy to final states with two $3p$ vacancies with LS designations of $^3P_{2,1,0}$, $^1D_2$, and $^1S_0$; 8 to states with $3s3p$ vacancies ($^3P_{2,1,0}$ and $^1P_0$); and 2 to states with two $3s$ vacancies ($^1S_0$). However, experimental measurements of the Auger spectrum show a much more complicated structure, and most of the work to date has attempted to elucidate the reasons for the additional structure. Basically these are the following.

(a) Initial-state correlation. The physical picture of the "normal" Auger spectrum described above assumes that *only* single vacancies occur in the initial excitation process. When initial-state correlation is included, multiple vacancy states will always be present in any excitation process and will lead to additional Auger transitions.

(b) Final-state core correlation. The final states of the *LMM* Auger process listed above are pure states only in an independent-particle model. When final-state core correlation is included, Auger transitions are possible to states with an additional $3s$ or $3p$ vacancy, with the excited electron either in a discrete (shakeup) or continuum (shakeoff) state. Of course, similar states may also be present due to initial-state correlation. In general, a multiconfiguration description of both initial and final ion states is necessary to represent accurately the observed spectra [2].

(c) Final-state continuum interactions. When a $L_{2,3}$ vacancy decays, electrons of different energies are ejected, corresponding to the energetically available final core states of the doubly charged ion. Interchannel coupling can occur between these various continuum channels and affect the observed Auger spectrum [3].

(d) Vacancy cascades. The correlation effects listed above can produce "satellite peaks" in both photoelectron and Auger spectra. In the case of Auger spectra, however, an additional mechanism is possible. When an inner electron is removed, vacancies can be transferred to outer subshells either by radiation or Auger processes. In the present case, provided the excitation energy is below the K excitation threshold [4], the only possible effects on the $L_{2,3}$ Auger spectrum will be the transfer of L_1 vacancies. Transfers via radiation to $L_{2,3}$ and $M_{2,3}$ will not produce any new spectral lines or modify the relative intensities observed in the spectra. However, Coster-Kronig processes can transfer a vacancy from L_1 to $L_{2,3}$ and produce additional M_1 and $M_{2,3}$ vacancies. Such vacancy transfers will result in satellite peaks in the observed Auger spectrum which could also be produced by electron shakeoff in either the initial ionization process or the Auger decay process.

Although there have been several measurements of the argon $L_{2,3}$ Auger spectrum using photon [5–7] and ion [8] impact to produce the initial $2p$ vacancies, the most definitive work has been done by electron impact [9–11]. Detailed studies [12,13] have been made of the $L_{2,3}M_{2,3}M_{2,3}$ spectrum between 200 and 210 eV, and good agreement with theoretical calculations was obtained. However, the spectrum at lower electron energies, corresponding to $L_{2,3}M_1M_{2,3}$ and $L_{2,3}M_1M_1$ transitions, is more complicated, since the intensity of satellite lines is comparable to that of the "normal" Auger transitions.

There have been a few definitive theoretical studies of the $L_{2,3}MM$ spectrum. McGuire [14] analyzed the $L_{2,3}MM$ spectrum of Ref. [11] and was able to explain most of the observed lines as due to Auger transitions with an additional vacancy in the M shell due either to shakeoff or transfer of L_1 vacancies via $L_1L_{2,3}M$ Coster-Kronig processes. His results are consistent with a ratio of 5% for the relative probability of forming $2s$ or $2p$ vacancies. Dyall and Larkins [15] have analyzed the spectrum assuming the dominant effect is final ionic state configuration interaction [(b) above]. Recently, Tulkki

et al. [16] have investigated the effects of final-state correlation [(b) and (c) above] on the $L_2M_{2,3}M_{2,3}$ transition rates, and Tulkki and Mäntykenttä [17] have studied relaxation effects.

It would be useful to separate vacancy transfer effects from those of configuration interaction. In principle, this could be done for the argon $L_{2,3}MM$ spectrum by using excitation energies just below the L_1 ionization potential but above the $L_{2,3}$ ionization potentials, as in Refs. [6] and [16], so that vacancy transfer is energetically not allowed. An alternative, which will be described here, is to increase the relative probability of forming $2s$ vacancies, which will provide an enhancement of the satellite spectra formed by the vacancy transfer process. This can be done by exciting L vacancies via photon impact at energies far above the L_1 ionization potential but below the K ionization potential. The satellite spectra in this case are enhanced principally due to the fact that the relative probability of forming $2s$ or $2p$ vacancies strongly increases with photon energy.

The outline of the remainder of the paper is as follows: Section II contains a brief discussion of the experimental procedure. Basically, this consists of observation of the $L_{2,3}MM$ Auger spectrum with photon excitation at incident energies of 3174 and 2200 eV and with electron-impact excitation at 2 and 4.5 keV. Section III contains a discussion of the various excitation and vacancy transfer processes and estimates of the rates for these processes. In Sec. IV the experimental results are compared with the theoretical calculations and with previous work. Finally, Sec. V is devoted to a summary of the results and suggestions for future work.

II. EXPERIMENT

Measurements were made using a double-pass cylindrical mirror analyzer (CMA) [18] on x-ray beamline X-24A [19] at the National Synchrotron Light Source. The x-ray beam passed through an effusive beam of Ar gas positioned at the source point of the CMA, and the CMA was positioned with its symmetry axis parallel to the polarization direction of the x-ray beam. The CMA was operated in retarding mode at 20 eV pass energy using 4-mm-diam internal apertures. Argon LMM Auger electron spectra were recorded over the kinetic-energy range 150–220 eV using 0.1-eV steps at an observed resolution of 0.7 eV full width at half maximum (FWHM). The intensities of the electron spectra varied linearly with Ar gas pressure, indicating an absence of gas-scattering effects. The electron spectra measured at beamline X-24A were recorded at a background pressure of 13 mPa.

The electron count rate in the kinetic-energy region of the Ar LMM Auger spectrum was observed to increase strongly as the x-ray energy was scanned from below to above the K edge, due to K-shell to L-shell vacancy cascade processes [4]. This effect was used to record excitation spectra of the electron count rate vs x-ray energy which appear similar to photoabsorption spectra of the Ar K edge [20–22]. The x-ray energy scale was referenced to the distinct $1s$ to $4p$ resonance located 2.72 eV below the $1s$ ionization edge [20,22]. Breinig *et al.* [20] have measured the argon K ionization energy to be 3206.3 ± 0.3 eV.

The Ar LMM Auger electron spectra shown in Figs. 1(a) and 1(b) were recorded using 3174 and 2200 eV x-ray energies. Si(111) crystals were used in the beamline's double-crystal monochromator, and we estimate that the energy bandwidths (FWHM) were ≈ 0.5 eV at 2200 eV x-ray energy and ≈ 0.8 eV at 3174 eV.

The CMA's internal electron gun [18] was also used to record Ar LMM Auger electron spectra using the same pass energy and step size as were used for the x-ray generated spectra. In the spectrum shown in Fig. 1(c) the electron gun was operated at 2000 eV beam energy and 18 μA beam current. A smaller Ar gas density (1.9 mPa background pressure) was used to prevent saturation of the electron counting circuit and to reduce the background due to gas scattering of the electron beam. An essentially identical Ar LMM spectrum (not shown) was recorded with the electron gun operated at 4500 eV beam energy and 16 μA beam current. This result indicates that relatively little K-shell excitation occurs via electron impact.

The Ar LMM electron spectra were placed on an absolute kinetic-energy scale by positioning the strong diagram line $L_3M_{2,3}M_{2,3}(^1D_2)$ at 203.5 eV. This kinetic energy is consistent with the energy reported by Werme,

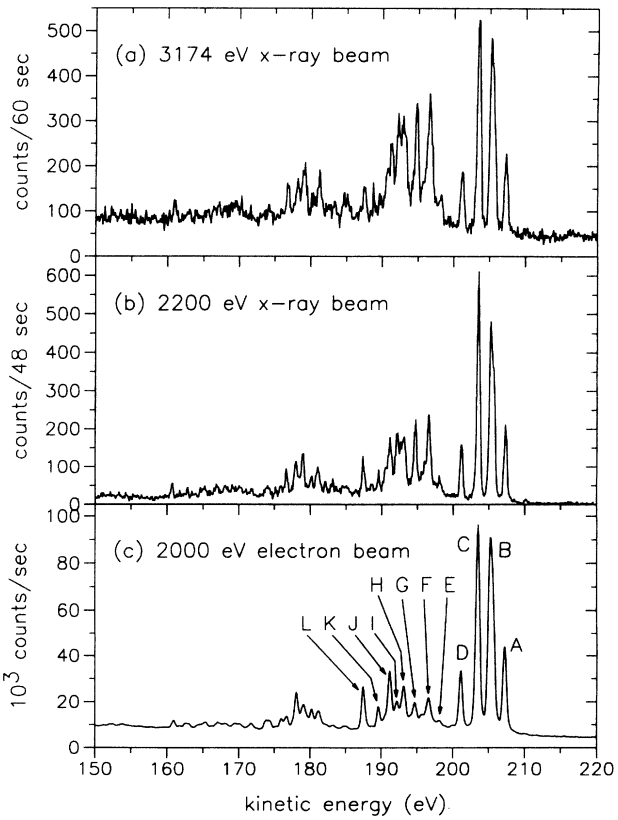

FIG. 1. The argon $L_{2,3}MM$ Auger spectrum recorded under different excitation conditions: (a) using 3174-eV x rays, (b) using 2200-eV x rays, and (c) using 2000-eV electron beam excitation.

Bergmark, and Siegbahn [11] and with the tabulated energies of the upper and lower levels involved in the Auger transition, that is, Ar^{+} $2p^{-1}(^2P_{3/2})$ [23] and Ar^{2+} $3p^{-2}(^1D_2)$ [24].

III. VACANCY TRANSFER PATHS AND DECAY RATES

With excitation energies below the K ionization threshold, multiple vacancies can arise either by correlation effects [(a), (b), and (c) above] or as a result of initial formation of an L_1 vacancy and transfer of this vacancy via an $L_1L_{2,3}M$ Coster-Kronig process. In order to predict the observed spectra, estimates must be made of the probabilities of initial formation of L_1, L_2, and L_3 vacancies, both by photon and electron impact, and also of the probability of additional vacancies being formed in the excitation process. Simple shakeoff theory [25] predicts that when an $L_{2,3}$ vacancy is formed, the probability of simultaneously forming an $M_{2,3}$ vacancy will be 13% and that of forming an M_1 vacancy will be less than 2%. For the electron-impact spectra of Werme, Bergmark, and Siegbahn [11], taken at 3–5 keV incident energy, McGuire [14] concluded that this estimate was too high and attempted to explain the observed $L_{2,3}MMM$ spectra as due to vacancy transfer via $L_1L_{2,3}M$ Coster-Kronig transitions. Here, essentially the same procedure will be followed, since in our data taken with monoenergetic photons, this appears to be the dominant mechanism for the formation of satellite Auger lines. The reason for this appears to be that at photon energies well above the L_1 threshold but below the K ionization threshold, L_1 photoionization is a considerable fraction of the total L cross section, as illustrated in Table I. This is in marked contrast to the case of electron impact, where the calculated ratio [26] is about 15% and the actual ratio is probably less than the calculated value. Table I shows that $2s$ ionization is actually more likely than $2p$ ionization at incident photon energies above 3 keV.

TABLE I. Ratios of the $2s$ cross section to $2p$ cross section at various energies from Ref. [27].

Photon energy (eV)	$\sigma_{2s}/(\sigma_{2p})$
1000	0.43
2000	0.86
3000	1.29
(K threshold)	1.36

The various decay processes for an L_1 vacancy and their relative rates are compared with Auger rates for $L_{2,3}$ vacancies in Table II. From the table it is apparent that the major decay path for an L_1 vacancy is via Coster-Kronig transitions, which will create $L_{2,3}$ vacancies with an additional M-shell vacancy. Radiative decay is negligible, and formation of two M-shell vacancies occurs only 5% of the time.

Based on the above estimates, we have used the following simple model to explain the spectra produced by photon and electron impact: It is assumed that the relative populations of the initially formed L_1, L_2, and L_3 vacancies are given by the calculated cross sections for subshell ionization of Refs. [26] and [27]. Radiative decay processes and shakeoff in the initial vacancy formation process are ignored. The relative population of L_1 vacancies is reduced by 5% to account for L_1MM Auger decay. Two spectra are then computed, i.e., the "normal" Auger spectrum for a single $L_{2,3}$ vacancy and the satellite spectrum which arises from decay of an $L_{2,3}$ vacancy with an additional M vacancy produced via vacancy transfer from an original L_1 vacancy.

In order to produce model spectra, the energies of the initial and final hole states must be estimated as well as the decay rate for each Auger transition. Initial estimates of the energies of the states involved, as well as the transition rates for each transition, were obtained by the

TABLE II. Vacancy transfer rates for L_1, L_2, and L_3 vacancies in argon (in units of 10^{-4} a.u.) from Refs. [27] and [28].

Radiative and Coster-Kronig			"Normal" $L_{2,3}$ processes		
Decay process	Final state	Rate 10^{-4} a.u.	Decay process	Final state	Rate 10^{-4} a.u.
Radiative	M_2	0.26			
	M_3	0.51			
Coster-Kronig	$L_1L_2M_1$	163	L_2MM	$L_2M_1M_1$	0.8
	$L_1L_2M_2$	67		$L_2M_1M_2$	11.9
	$L_1L_2M_3$	76		$L_2M_1M_3$	0.9
	$L_1L_3M_1$	326		$L_2M_2M_2$	10.1
	$L_1L_3M_2$	76		$L_2M_2M_3$	36.7
	$L_1L_3M_3$	190		$L_2M_3M_3$	1.0
L_1MM	$L_1M_1M_1$	9.1	L_3MM	$L_3M_1M_1$	0.8
	$L_1M_1M_2$	17.6		$L_3M_1M_2$	0.5
	$L_1M_1M_3$	28.4		$L_3M_1M_3$	12.4
	$L_1M_2M_2$	0.3		$L_3M_2M_2$	0.2
	$L_1M_2M_3$	0.1		$L_3M_2M_3$	19.1
	$L_1M_3M_3$	0.7		$L_3M_3M_3$	28.7

relativistic version of Cowan's atomic structure program [29]. For most of the Auger transitions, more accurate energies of the initial and final states could be obtained from experimental data [23,24]. These experimental energies were used whenever possible, but the decay rates were estimated either from the Hartree-Fock structure calculations or from McGuire's Hartree-Fock-Slater results [14].

IV. EXPERIMENTAL AND THEORETICAL RESULTS

A. The "normal" $L_{2,3}MM$ spectrum

The $L_{2,3}MM$ spectrum has been measured many times [5–13] and, with one exception, can be considered completely characterized. The $L_{2,3}M_{2,3}M_{2,3}$ spectrum, in particular, has been studied in detail, and although all of the expected lines are not resolved, the positions and intensities of the observed lines are well known.

The $L_{2,3}M_1M_{2,3}$ and $L_{2,3}M_1M_1$ spectra have also been measured several times. Since the $L_{2,3}$ binding energies are well known [23] and the final-state energies corresponding to $L_{2,3}M_1M_{2,3}$ transitions are also known [24], accurate predictions can be made of the energies of these transitions. These are shown in Table III along with the results of earlier measurements and our results from the electron-impact spectrum [Fig. 1(c)].

The final-state energies corresponding to $L_{2,3}M_1M_1$ transitions are not known, and it is uncertain whether or not these transitions have been observed in the Auger spectrum. These two transitions were first reported in Ref. [10] to be at 179.93 and 177.79 eV. The later work of Ref. [11] placed them at 180.06 and 177.91 eV. However, McGuire [14] pointed out that the intensity of these transitions were much larger than that calculated, and on that basis reassigned these two transitions to those observed in Ref. [11] at 176.32 and 174.22 eV. Dyall and Larkins [15] concurred with this assignment. Their calculations predicted a shift of the position of the $^1S_0$ state with two $3s$ vacancies relative to the $^1S_0$ state with two $3p$ vacancies of approximately 10 eV and a loss in intensity for the $L_{2,3}M_1M_1$ transitions due to the interaction between the two configurations. However, even with configuration interaction included, there is a relative uncertainty of about 1–2 eV in the calculations of the positions of the levels. In view of this, it would appear impossible to definitely assign these transitions to any of the number of lines observed in this energy range in the high-resolution work of Ref. [11].

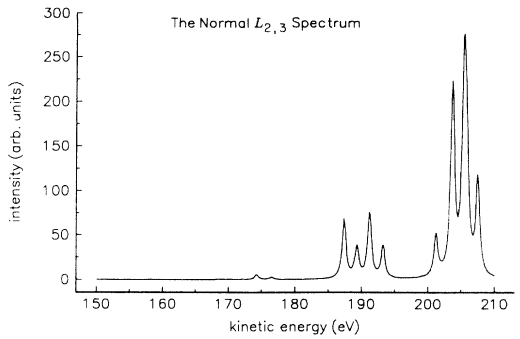

FIG. 2. The normal $L_{2,3}MM$ model spectrum. Each spectral line has been convoluted with a Lorentzian of 0.34 eV FWHM.

Figure 2 shows a model $L_{2,3}MM$ spectrum obtained in the following manner: The calculated Hartree-Fock intensities were used for each transition, but the energies of each transition were taken from the spectroscopic values of Table III, with the exception of the $L_{2,3}M_1M_1$ transitions, which were taken to be at 176.32 and 174.22 eV. The line spectrum was then convoluted with a Lorentzian of 0.34 eV FWHM. Note that this width is smaller than the measured widths of the experimental spectra in Fig. 1, and was chosen since a Lorentzian profile was used to model both the natural width of the lines (0.13 eV) and the experimental resolution.

Figure 2 indicates two things. First, the relative intensities of the $L_{2,3}M_{2,3}M_{2,3}$ transitions differ from experiment. The major difference is that the calculations predict that the ^3P components are the largest, whereas all experiments show that the ^1D components are the largest. This accounts for the reversal of the relative intensities of peaks B and C in the experimental spectra of Fig. 1 compared with the calculated spectrum in Fig. 2. The calculated relative intensities agree rather well with those of McGuire [14] and of Dyall and Larkins [15], although the former calculation is based on a simpler model and the latter includes some final-state configuration interaction. Second, Fig. 2 shows that the intensity of the

TABLE III. Energies (in eV) of the $L_{2,3}M_1M_{2,3}$ spectrum from various sources. Uncertainties in the present measurements are estimated to be ±0.3 eV.

Level	Atomic spectra (Ref. [24])	Ref. [10]	Ref. [11]	This paper
L_3-$^1P_1$	187.20	187.16	187.33	187.5
L_3-$^3P_0$	190.76			
L_3-$^3P_1$	190.83	190.76		
L_3-$^3P_2$	190.95	190.91	191.13	191.2
L_2-$^1P_1$	189.06	189.30	189.49	189.6
L_2-$^3P_0$	192.97	192.84	193.02	
L_2-$^3P_1$	192.99	192.90	193.13	193.2
L_2-$^3P_0$	193.11			

TABLE IV. Upper and lower limits of the energies (in eV) for the transfer Auger spectra.

	Final configuration		
Initial configuration	$3s^23p^3$	$3s3p^4$	$3s^03p^5$
$2p^53s3p^6$		189.4–198.7	177.0–178.8
$2p^53s^23p^5$	190.1–200.9	172.4–186.3	160.3–166.8

$L_{2,3}M_1M_1$ transitions is so low that they may be masked by transitions due to other processes.

B. The L_1-$L_{2,3}$ transfer spectrum

If an L_1 vacancy is created, Coster-Kronig transitions can leave a doubly charged ion in $2p^53s3p^6$ or $2p^53s^23p^5$ configurations, which can subsequently decay into the triply ionized configurations $3s^23p^3$, $3s3p^4$, and $3s^03p^5$. Thus, there will be a number of satellite Auger transitions in the same energy range as the normal $L_{2,3}MM$ spectrum. There will be ten states in the configuration $2p^53s^23p^5$ and four for $2p^53s3p^6$ which will be the initial states of the transfer Auger spectrum. The $2p^53s^23p^5$ states can decay to $3s^23p^3$ (five states), $3s3p^4$ (eight states), or $3s^03p^5$ (two states), and $2p^53s3p^6$ can decay to $3s3p^4$ or $3s^03p^5$. The final-state energies of the $3s^23p^3$ and $3s3p^4$ configurations are known from spectroscopic data [24] in relation to the ground state of atomic argon. The energies of the initial-state configurations are not known as precisely. However, it is possible to make good estimates. Mehlhorn [30] has made a careful analysis of the Coster-Kronig spectrum between 25 and 50 eV and could assign energies to the transitions from the initial L_1 vacancy state, with an uncertainty of approximately 0.5 eV. The $2s$ binding energy has recently been measured as 326.25±0.05 eV [31]. Using this value and Mehlhorn's data, the energies of the final states of the Coster-Kronig transitions can be estimated, and, with the data from Ref. [24], the energies of most of the transfer Auger transitions can be determined. The range of values of expected Auger lines obtained by this procedure is given in Table IV. As is the case with the normal Auger spectrum, the only values that cannot be obtained by this procedure are the energies corresponding to final states of the configuration $3s^03p^5$, since no information from atomic spectroscopy is available for these two states. In Table IV, the estimate of the range of energies corresponding to these final states is made by assuming, as was done in Ref. [14], that their center of gravity lies 12.5 eV above the $3s3p^4\ ^2S$ term.

In order to estimate the transfer Auger spectrum, the branching ratios for the $L_1L_{2,3}M$ Coster-Kronig transitions must be known, as well as the relative intensities for the subsequent Auger transitions. These values were obtained from the calculated rates for each transition. Figure 3 shows the calculated transfer Auger spectrum in the energy range between 150 and 210 eV. The spectrum was obtained by estimating the energy and relative intensity of each transition and convoluting the spectrum with a Lorentzian whose FWHM was set equal to the calculated decay width of the initial state plus 0.2 eV to approximate the experimental resolution. Figure 3 shows that the transfer spectrum has most of its intensity in the energy ranges 174–181 and 189–200 eV, with some intensity in the 159–162-eV range, which is due to $2p^53s^23p^5$-$3s^03p^5$ transitions. Note that at the resolution used to construct the spectrum, it is impossible to assign peaks to individual transitions, since the spacing of the various transitions is in many cases smaller than the sum of the natural linewidth, which varies from 0.05 to 0.25 eV, and the 0.2 eV used to account for experimental resolution. In view of the complexity of the transfer Auger spectrum and the fact that the experimental spectra were obtained at moderate resolution, no attempt will be made here to assign peaks to specific transitions.

The observed spectra will contain components of the normal spectrum and of the transfer spectrum in addition to components from direct two-electron excitation processes. The relative weight of the normal and transfer components will depend on the relative probability of forming a $2s$ or $2p$ vacancy. If K is the ratio of the $2s$ and $2p$ cross sections as shown in Table I, the weights for the "normal" and "transfer" spectra will be $1/(1+K)$ and $K/(1+K)$, respectively. Figures 4–6 show composite spectra corresponding to $K=0.2$, 0.8, and 1.2, which are to be compared with the experimental spectra in Fig. 1. In Figs. 4–6 the portion of the spectrum due to the normal Auger spectrum is shown as a dotted line. Figure 4 ($K=0.2$), which should be comparable to the electron-impact spectrum in Fig. 1(c), shows how vacancy transfer affects the spectrum. There is, of course, no effect on the major part of the spectrum above 201 eV. However, new peaks of comparable intensity to those of the "normal" spectrum appear in the 185–200-eV range, and the apparent intensity of the four normal spectral peaks is

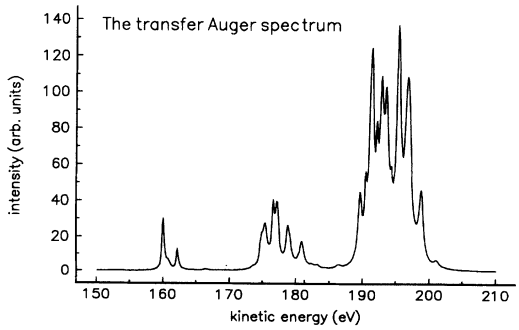

FIG. 3. The transfer Auger $L_{2,3}MM$ model spectrum arising from an initial L_1 vacancy. Each spectral line has been convoluted with a Lorentzian of FWHM equal to 0.2 eV plus the natural width of the line.

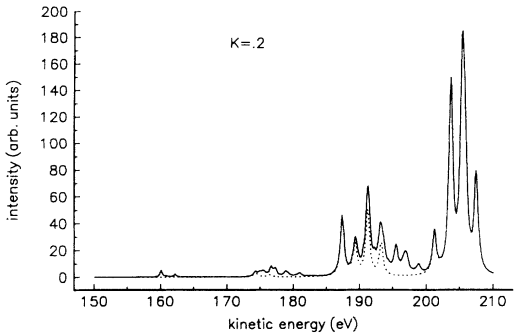

FIG. 4. Composite spectrum corresponding to a ratio of $2s$ to $2p$ initial vacancies of 0.2. The solid line is the composite spectrum and the dotted line is the contribution of the normal Auger spectrum.

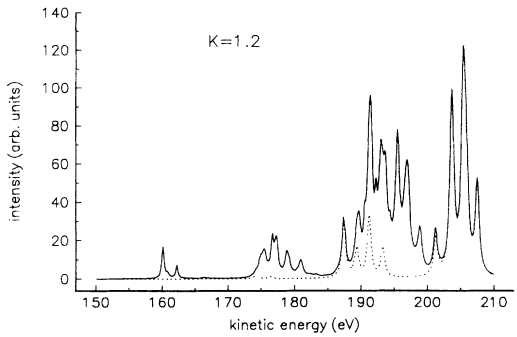

FIG. 6. Composite spectrum corresponding to a ratio of $2s$ to $2p$ vacancies of 1.2.

modified. The "normal" spectrum peaks near 175 eV are still present but are less intense than structure due to the transfer spectrum. Structure also appears in the 160–163-eV range.

Comparison of this model spectrum (Fig. 4) with Fig. 1(c) indicates the inadequacies of the model. As is the case for the "normal" spectrum in the 200–210-eV range, the calculation does not give correct intensities. However, in the range 185–200 eV, all of the peaks identified in Fig. 1(c) are accounted for and have approximately the same relative intensities in both figures. The calculation does not reproduce the four peaks shown in Fig. 1(c) in the 178–182-eV range. This is reasonable, since transitions in this energy range have been identified as "shake-up" satellites, with one $3p$ electron being promoted to a $3d$ or $4s$ orbital [11]. Figures 5 and 6, which should be comparable to the x-ray generated spectra obtained at 2200 and 3174 eV, respectively, clearly indicate that the principal reason for the change in intensity in the energy range below 200 eV is due to the transfer Auger spectrum. For K values greater than 1, i.e., more $2s$ than $2p$ vacancies formed, the transfer spectrum in the 185–200-eV range will be of comparable intensity to the normal spectrum in the 200–210-eV range, as is observed in Fig. 1(a).

The variation of intensity with excitation energy can be used to sort out which peaks in the observed spectra are due to the initial excitation process and which are the result of the transfer of vacancies from one subshell to another. In the present case, an example of how this can be done is given in Table V, which lists the 12 highest energy peaks indicated in Fig. 1(c) and compares the peak heights with those of Fig. 1(a). In this comparison, the peak height ratio for the strongest line (peak C) at 203.5 eV is normalized to 1.0. With this normalization, the ratio of the peak heights for peaks A–D, i.e., the $L_{2,3}M_{2,3}M_{2,3}$ spectrum, is approximately 1, indicating that there is no contribution from the transfer spectrum to these peaks. The four peaks which correspond to diagram transitions to sp^5 final states (H, J, K, and L) also have low values, with the exception of peak H. These values are consistent with the results shown in Fig. 6, which shows that peak L has almost no contribution from the transfer spectrum, whereas there are contributions to the other peaks. The remaining peaks (E, F, G, and I), with large peak height ratios, must then be due to the transfer Auger spectrum.

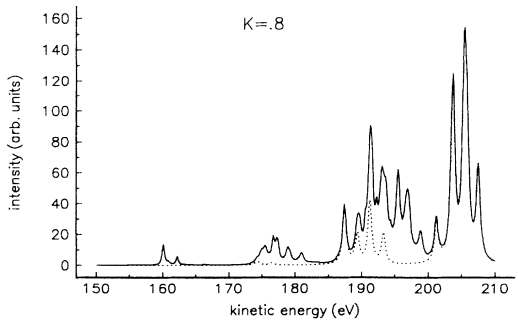

FIG. 5. Composite spectrum corresponding to a ratio of $2s$ to $2p$ vacancies of 0.8.

TABLE V. The highest energy peaks observed in the electron-impact spectrum [Fig. 1(c)] and the ratios of the peak heights of corresponding peaks in the 3174-eV x-ray data [Fig. 1(a)] to those of the electron-impact data and normalized to 1.0 for peak C. Uncertainties in the energies and peak height ratios are estimated to be ±0.3 eV and ±10%, respectively.

Peak	Energy (eV)	Ratio
A	207.2	0.8
B	205.2	1.0
C	203.5	1.0
D	201.2	1.0
E	198.1	2.1
F	196.6	3.1
G	194.7	3.2
H	193.2	2.1
I	192.2	2.9
J	191.2	1.4
K	189.6	1.4
L	187.5	1.0

V. SUMMARY AND SUGGESTIONS FOR FUTURE WORK

Although the argon $L_{2,3}MM$ Auger spectrum has been studied extensively, it is still not completely understood. The key result of this paper is the realization that cascade processes can produce major excitation-dependent modifications in the observed spectra. This invalidates the assumption that any transitions observed in addition to the diagram lines must be due to multiple excitations. Studies of the transfer Auger spectrum offer the advantage that it can be characterized by its dependence on excitation conditions. There seem to be two promising directions for future work in this area. In order to completely characterize the "normal" Auger spectrum and its associated satellites, excitation energies below the 2*s* excitation threshold should be used, as in Refs. [6] and [16]. Spectra taken at high resolution under these conditions would be completely free of cascade effects and thus would reflect correlation effects in the initial vacancy creation process or in the final states. As a followup to the present work, it would be useful to repeat the photon measurements at higher electron-energy resolution and at several excitation energies. This would provide more information on the transfer Auger spectrum to possibly separate out those effects due to transfer from those due to multielectron excitation.

ACKNOWLEDGMENTS

The measurements were made in part at the National Synchrotron Light Source, Brookhaven National Laboratory, which is supported by the U. S. Department of Energy, Division of Materials Sciences and Division of Chemical Sciences. J. W. C. acknowledges support from OPM under Contract No. CSA-3115486. The work was supported in part by the U. S. Department of Energy, Office of Basic Sciences, under Contract No. W-31-109-Eng-38.

[1] W. Mehlhorn, in *Atomic Inner Shell Physics,* edited by B. Crasemann (Plenum, New York, 1985), Chap. 4.
[2] R. L. Martin and D. A. Shirley, J. Chem. Phys. **64**, 3685 (1976).
[3] S. T. Manson, J. Electron Spectrosc. Relat. Phenom. **9**, 21 (1976).
[4] Auger spectra have also been taken at photon energies above the *K* edge: S. H. Southworth, M. A. MacDonald, T. LeBrun, and Y. Azuma (unpublished).
[5] G. Johansson, J. Hedman, A. Berndtsson, M. Klasson, and R. Nilsson, J. Electron Spectrosc. Relat. Phenom. **2**, 295 (1973).
[6] H. Aksela and S. Aksela, J. Phys. (Paris) Colloq. **48**, C9-565 (1987).
[7] J. A. de Gouw, J. van Eck, J. van der Weg, and H. G. M. Heideman, J. Phys. B **25**, 2007 (1992).
[8] D. J. Volz and M. E. Rudd, Phys. Rev. A **2**, 1395 (1970).
[9] K. Siegbahn, C. Nordling, G. Johansson, J. Hedman, P. F. Heden, K. Hamrin, U. Gelius, T. Bergmark, L. O. Werme, R. Manne, and Y. Baer, *ESCA Applied to Free Molecules* (North-Holland, Amsterdam, 1969).
[10] W. Mehlhorn and D. Z. Stalherm, Z. Phys. **217**, 294 (1968).
[11] L. O. Werme, T. Bergmark, and K. Siegbahn, Phys. Scr. **8**, 149 (1973).
[12] D. Ridder, J. Dieringer, and N. Stolterfohlt, J. Phys. B **9**, L307 (1976).
[13] J. Vayrynen and S. Aksela, J. Electron Spectrosc. Relat. Phenom. **16**, 423 (1979).
[14] E. J. McGuire, Phys. Rev. A **11**, 1880 (1975).
[15] K. G. Dyall and F. P. Larkins, J. Phys. B **15**, 2793 (1982).
[16] J. Tulkki, T. Åberg, A. Mäntykenttä, and H. Aksela, Phys. Rev. A **46**, 1357 (1992).
[17] J. Tulkki and A. Mäntykenttä, Phys. Rev. A **47**, 2995 (1993).
[18] P. W. Palmberg, J. Vac. Sci. Technol. **12**, 379 (1975).
[19] P. L. Cowan, S. Brennan, R. D. Deslattes, A. Henins, T. Jach, and E. G. Kessler, Nucl. Instrum. Methods A **246**, 154 (1986); P. L. Cowan, S. Brennan, T. Jach, D. W. Lindle, and B. A. Karlin, Rev. Sci. Instrum. **60**, 1603 (1989).
[20] M. Breinig, M. H. Chen, G. E. Ice, F. Parente, B. Crasemann, and G. S. Brown, Phys. Rev. A **22**, 520 (1980).
[21] R. D. Deslattes, R. E. LaVilla, P. L. Cowan, and A. Henins, Phys. Rev. A **27**, 923 (1983).
[22] T. Watanabe, Phys. Rev. **139**, A1747 (1965).
[23] G. C. King and F.H. Read, in *Atomic Inner-Shell Physics,* edited by B. Crasemann (Plenum, New York, 1985), pp. 317–375.
[24] C. E. Moore, *Atomic Energy Levels,* Natl. Bur. Stand. (U.S.) Circ. No. 467 (U.S. GPO, Washington, D.C., 1949), Vol. I.
[25] T. A. Carlson and C. W. Nestor, Jr., Phys. Rev. A **8**, 2887 (1973).
[26] S. J. Wallace, R. A. Berg, and A. E. S. Green, Phys. Rev. A **7**, 1616 (1972).
[27] J. H. Scofield, Lawrence Livermore Laboratory Report No. UCRL-51231, 1972 (unpublished); Laboratory Report No. UCRL-51326, 1973 (unpublished).
[28] E. J. McGuire, Phys. Rev. A **3**, 1801 (1971).
[29] This program may be obtained from Los Alamos via ftp (file transfer protocol). We would like to thank Dr. R. Cowan for making the program available to interested users.
[30] W. Mehlhorn, Z. Phys. **208**, 1 (1968).
[31] P. Glans, R. E. LaVilla, M. Ohno, S. Svensson, G. Bray, N. Wassdahl, and J. Nordgren, Phys. Rev. A **47**, 1539 (1993).